

Resistance switching at the interface of LaAlO₃/SrTiO₃

Y. Z. Chen,^{1,a)} J. L. Zhao,² J. R. Sun,² N. Pryds,¹ and B. G. Shen²

¹Fuel Cells and Solid State Chemistry Division, Risø National Laboratory for Sustainable Energy, Technical University of Denmark, Roskilde 4000, Denmark

²State Key Laboratory of Magnetism, Institute of Physics and Beijing National Laboratory for Condensed Matter Physics, Chinese Academy of Sciences, Beijing 100190, People's Republic of China

(Received 2 August 2010; accepted 26 August 2010; published online 20 September 2010)

At the interface of LaAlO₃/SrTiO₃ with film thickness of 3 unit cells or greater, a reproducible electric-field-induced bipolar resistance switching of the interfacial conduction is observed on nanometer scale by a biased conducting atomic force microscopy under vacuum environment. The switching behavior is suggested to be an intrinsic feature of the SrTiO₃ single crystal substrates, which mainly originates from the modulation of oxygen ion transfer in SrTiO₃ surface by external electric field in the vicinity of interface, whereas the LaAlO₃ film acts as a barrier layer. © 2010 American Institute of Physics. [doi:10.1063/1.3490646]

The discovery of the metallic conduction at the interface between two insulating oxides, LaAlO₃ (LAO) and SrTiO₃ (STO),¹ has attracted intensive attention in recent years.²⁻⁹ However, no consensus on its origin has been achieved.³ The polar catastrophe induced electronic reconstruction,^{1,2} the oxygen vacancies dominated conduction,⁴ or the extrinsic doping by La-interdiffusion at interface,⁵ all can explain the conducting behavior. Nevertheless, it has been generally accepted that the conduction is confined to the interface in samples grown under an oxygen pressure range of $1.0 \times 10^{-5} < P_{O_2} < 1.0 \times 10^{-4}$ mbar.² Meanwhile, the interfacial conducting behavior depends critically on LAO film thickness d .⁶ The metallic conducting heterointerface appears only when d reaches a critical value of 4 unit cells (uc), below which the interface remains insulating. Interestingly, when $d=3$ uc, the insulating interface could be turned to be conducting by external electric field.⁶ Furthermore, this electric-field controlled interfacial metal-insulator (MI) transition can also be realized at nanometer scales by means of a conducting atomic force microscopy (CAFM) probe.⁷ These findings show application potentials in oxide electronic devices,^{8,9} however, their underlying mechanisms are also not clarified unambiguously. In this letter, besides the electric-field controlled interfacial MI transition at $d=3$ uc in air, a reproducible resistance switching of the interfacial conductance is observed for $d \geq 3$ uc samples in a vacuum environment, which is proposed to originate from the modulation of oxygen ion transfer in STO by external electric field near the interface.

The LAO films were deposited by pulsed laser deposition from a single crystalline LAO target on TiO₂-terminated (001) STO substrates.¹⁰ During deposition, a substrate temperature of 750 °C and an oxygen pressure of 2.0×10^{-5} mbar were used. The film growth process was monitored by high-pressure reflective high energy electron diffraction (RHEED). Clear RHEED intensity oscillations, indicating a layer-by-layer film growth mode, were observed and were used to determine the film thickness d . After film deposition, the samples were cooled down to room temperature under deposition oxygen pressure. CAFM measurements

were performed at room temperature on three samples with $d=1, 3,$ and 6 uc both in air and in high vacuum with a background pressure of 1.0×10^{-6} mbar.

A schematic illustration of the CAFM measurement is shown in Fig. 1(a), a conducting PtIr-coated tip, which acts as a mobile electrode, is grounded, and the voltage is applied laterally to the other electrode of deposited Cu on the surface. Before conducting measurements, the morphology of the samples is checked by AFM. All samples show an atomically flat terrace surface with terrace height of about 0.4 nm, as shown in Fig. 1(b). As a preliminary study of the interfacial conduction, we measured, in air, the local current-voltage (I - V) curves of the lateral structure with a current compliance of 100 pA (determined by our external current amplifier) by positioning the tip at different points. No current is detected under various applied voltage between -10 and $+10$ V for the sample with $d=1$ uc, suggesting a highly insulating interface state. While, for the sample with $d=6$ uc, a sharp current increase is obtained once the amplitude of applied voltage is increased to about 5 V. Fixed point measurements show a symmetric nonlinear I - V curve when sweeping voltage in the sequence of $0 \rightarrow -7$ V $\rightarrow 0 \rightarrow 7$ V $\rightarrow 0$ as shown in Fig. 2(a), and no obvious hysteresis is found in I - V curves. These results indicate that the interface is highly conductive,^{2,3} and that the measured currents may be dominated by electron tunneling currents through the LAO barrier layer. As for the sample with $d=3$ uc, no current is measured when a positive voltage is applied, even the voltage is up to $+10$ V, which indicates an insulating state of the

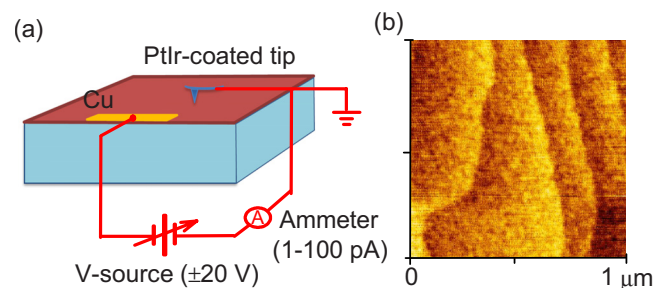


FIG. 1. (Color online) (a) Schematic diagram of the CAFM measurement. (b) A typical AFM morphology of the LAO/STO samples with terrace-structure, the terrace height is about 0.4 nm.

^{a)}Electronic mail: yunc@risoe.dtu.dk.

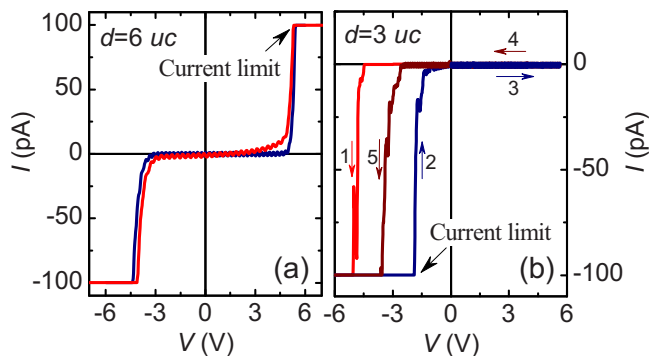


FIG. 2. (Color online) Typical I - V curves for LAO/STO in air with (a) $d=6$ uc and (b) $d=3$ uc. The numbers in (b) show the sequence of the applied voltage.

interface. However, a high enhancement of current appears once a negative voltage above the threshold value of -4.5 V is applied, which suggests the occurrence of the field-induced MI transition as previously reported.⁷ More interestingly, an asymmetric hysteresis I - V curve is clearly observed when sweeping voltage in the sequence of $0 \rightarrow -6$ V $\rightarrow 0 \rightarrow 6$ V $\rightarrow 0$ during fixed point measurements as shown in Fig. 2(b). The hysteretic I - V curve becomes nearly stable in the following measurements with the threshold voltage for current booming reduced to about -3.5 V. However, no current is detected under positive voltages during all the measurement processes. In addition, it is found that increasing the positive voltage to higher than $+6$ V will result in obvious changes in the surface morphology for this $d=3$ uc sample. Note that no obvious morphology changes are observed in all other measurements.

Though no current is measured under any positive voltage even after the appearance of negative-voltage induced MI transition in $d=3$ uc sample, the hysteresis in I - V curve generally implies a nonvolatile resistance switching behavior in transition metal oxides.¹¹ To understand its reason and to exclude the possibility of surface contamination, similar investigations are also performed in vacuum. Consistent with the results in air, the vacuum I - V measurements also show no interfacial conduction for $d=1$ uc sample. However, the application of voltage pulses in vacuum produces profound changes in the I - V characteristics of both samples with $d=3$ and 6 uc. The most striking feature of the I - V curves is the appearance of obvious hysteresis in both samples when sweeping voltage between negative and positive values during fixed point measurements. As shown in Figs. 3(a) and 3(b), applying a negative bias to the electrode up to a threshold value (-2.8 V for $d=6$ uc, -3.9 V for $d=3$ uc) markedly increases the interfacial conductance, and leads to the appearance of nearly symmetric I - V curves. While, a large positive voltage ($+4$ V for $d=6$ uc, $+9$ V for $d=3$ uc) can turn the interface back to a high resistance state. Moreover, this switching behavior is highly reproducible even after several cycles. Figures 3(c) and 3(d) show the current distribution maps of a scanned sample with $d=6$ uc under different biases. After scanning the tip linearly on the surface with a bias of -5 V, low resistance lines with a width of about 10 nm appear under the scanned area (reading voltage of $+2$ V) while leaving the other areas unaffected [Fig. 3(c)]. This low resistance state could be latter removed by a positive bias of $+5$ V applied perpendicularly to the low resistance lines as

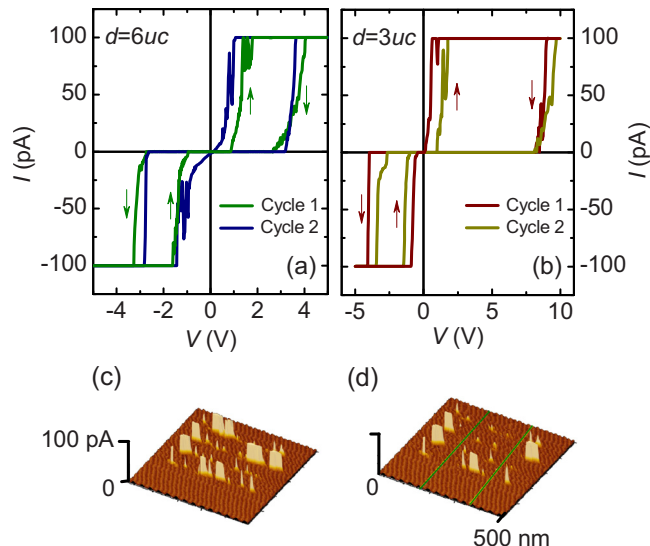


FIG. 3. (Color online) (a) and (b) show the typical I - V curves for LAO/STO in vacuum with $d=6$ uc and $d=3$ uc, respectively. (c) and (d) show the current images of $d=6$ uc after parallel linear scanning under -5 V and a followed perpendicular linear scanning under $+5$ V, respectively. The reading voltage is $+2$ V. The lines in (d) show the direction of the perpendicular linear scanning.

shown in Fig. 3(d), and could also be further turned back by applying the negative bias of -5 V again. Obviously, by sweeping the voltage between positive and negative bias, bipolar and nonvolatile resistance switching could be realized at the LAO/STO interface for $d \geq 3$ uc in vacuum.

The resistive switching effect has been observed in a wide variety of transition metal oxides,¹¹⁻¹⁵ the origin of which relies on the interplay of ionic and electronic conduction. Generally, the attracting and repelling of oxygen vacancies by applied voltage pulses constitutes the core process of this resistance switching,¹¹ which leads to the changes in the valence state of the transition metal cations and the electronic conductivity. Considering the facts that no valence-change metal-cation presents in LAO films, and that the resistance switching behavior for $d=6$ uc is quite similar to those observed in a metallic oxygen-deficient STO single crystal,¹⁴ which is also only possible under vacuum conditions, the resistance switching at the LAO/STO interface may mainly result from STO substrate with oxygen vacancies near the interface, as shown in Fig. 4(a). Under this assumption, the resistance switching can be understood as follows: when a large negative voltage is applied to the Cu electrode, the oxygen ions (O^{2-}) will be repelled to the tip, i.e., the anode. Meanwhile, the oxygen vacancies, which act as donors in STO, will accumulate under the electrode (cathode) area and propagate toward the tip to form highly conducting filaments that result in the formation of a lower resistance state, as illustrated in Fig. 4(b). This low resistance state will be kept until a large positive voltage pulse is applied to the Cu electrode. Then, the oxygen ions are attracted nearby and removed some oxygen vacancies beneath the electrode, which finally cuts the conducting filaments and results in a high resistance state, as illustrated in Fig. 4(c). Additionally, due to the presence of the LAO layer, the LAO/STO interface resembles greatly an oxide dual-layer memory element.¹⁵ The movement of oxygen ion under negative/positive voltage pulses will also lead to depletion/accumulation of negatively charged oxygen ions in the LAO

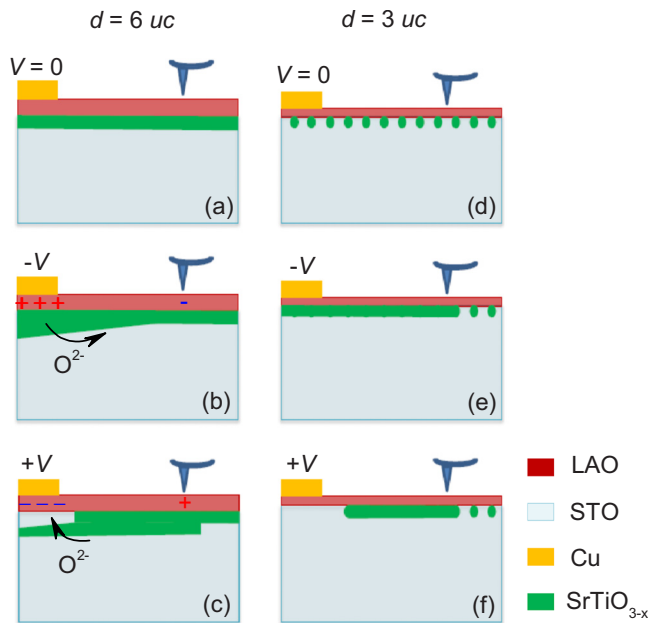


FIG. 4. (Color online) Sketched cross-sections of the electric-field controlled resistance switching at the interface of LAO/STO for $d=6$ uc [(a)–(c)] and $d=3$ uc [(d)–(f)].

film, which acts as a tunneling barrier layer. This will result in a reduction/enhancement of the effective height of the tunnel barrier, thus a contribution to the low/high resistance switching behavior. Therefore, the resistance switching at the interface of LAO/STO should be a consequence of the combination effects of both field-induced oxygen vacancies redistribution and field-modulated tunnel barrier height change. However, since the change in the tunnel barrier height will result in a smooth resistance variation,¹⁵ the observed abrupt resistance change strongly suggests that the oxygen vacancies redistribution in STO plays a dominant role in determining the resistance switching at the interface of LAO/STO. This is also consistent with the fact that a nearly symmetric I - V curve is observed when the interface is switched to a low resistance state as shown in Figs. 3(a) and 3(b).

The resistance switching for the insulating sample of $d=3$ uc is rather interesting, which may suggest the existence of oxygen vacancies in the initial state of the interface as shown in Fig. 4(d). If this is the fact, the oxygen vacancies should form in localized point defects at STO side, resulting in the insulating interface. Under negative voltage pulses, these point defects could be accumulated to line defects, such as dislocations,¹⁴ and lead to the conducting interface and thus resistive switching behavior as illustrated in Figs. 4(e) and 4(f). Compared to the case of $d=6$ uc with an initial conducting state, it is reasonable that a larger negative threshold voltage is needed here to accumulate the isolated

oxygen vacancies, as observed in Fig. 3(b). Meanwhile, the larger positive voltage needed to switch the interface back to a high resistance state may result from the formed thinner conducting layer. Assuming this scenario, the electric-field-induced MI transition at $d=3$ uc in air⁷ may be a hint of the oxygen-vacancies-dominated resistance switching behavior. Furthermore, the conducting behavior^{2,3} and the thickness dependent interfacial MI transition at $d=4$ uc (Ref. 6) in LAO/STO can also be explained by the oxygen vacancies evolution in STO from point defects to linear dislocations, whereas the oxygen vacancies may be triggered by the film growth process as shown in our recent researches.¹⁶

In summary, a reproducible and bipolar electric-field-induced nanoscale resistance switching is observed at the interface of LAO/STO with $d \geq 3$ uc by a CAFM under vacuum environment. The switching behavior is suggested to mainly originate from the modulation of oxygen ion transfer in STO layer by external electric field in the vicinity of interface, whereas the LAO films acts as a barrier layer.

We thank A. D. Wei, T. Y. Zhao, J. Y. Liu, F. B. Saxild, and J. Geyti for their technical help. J.R.S. and B.G.S. acknowledge the support from the National Basic Research of China, the National Natural Science Foundation of China, the Knowledge Innovation Project of the Chinese Academy of Science, and the Beijing Municipal Nature Science Foundation.

¹A. Ohtomo and H. Y. Hwang, *Nature (London)* **427**, 423 (2004).

²J. Mannhart, D. H. A. Blank, H. Y. Hwang, A. J. Millis, and J. M. Triscone, *MRS Bull.* **33**, 1027 (2008).

³S. A. Chambers, *Adv. Mater. (Weinheim, Ger.)* **22**, 219 (2010).

⁴G. Herranz, M. Basletic, M. Bibes, C. Carretero, E. Tafra, E. Jacquet, K. Bouzehouane, C. Deranlot, A. Hamzic, J.-M. Broto, A. Barthelemy, and A. Fert, *Phys. Rev. Lett.* **98**, 216803 (2007).

⁵P. R. Willmott, S. A. Pauli, R. Herger, C. M. Schlepütz, D. Martocchia, B. D. Patterson, B. Delley, R. Clarke, D. Kumah, C. Cionca, and Y. Yacoby, *Phys. Rev. Lett.* **99**, 155502 (2007).

⁶S. Thiel, G. Hammerl, A. Schmehl, C. W. Schneider, and J. Mannhart, *Science* **313**, 1942 (2006).

⁷C. Cen, S. Thiel, G. Hammerl, C. W. Schneider, K. E. Andersen, C. S. Hellberg, J. Mannhart, and J. Levy, *Nature Mater.* **7**, 298 (2008).

⁸C. Cen, S. Thiel, J. Mannhart, and J. Levy, *Science* **323**, 1026 (2009).

⁹R. Jany, M. Breitschaft, G. Hammerl, A. Horsche, C. Richter, S. Paetel, J. Mannhart, N. Stucki, N. Reyren, S. Gariglio, P. Zubko, A. D. Caviglia, and J.-M. Triscone, *Appl. Phys. Lett.* **96**, 183504 (2010).

¹⁰Y. Z. Chen and N. Pryds, *Thin Solid Films* (to be published).

¹¹R. Waser and M. Aono, *Nature Mater.* **6**, 833 (2007).

¹²Y. Watanabe, J. G. Bednorz, A. Bietsch, C. Gerber, D. Widmer, A. Beck, and S. J. Wind, *Appl. Phys. Lett.* **78**, 3738 (2001).

¹³D. Choi, D. Lee, H. Sim, M. Chang, and H. Hwang, *Appl. Phys. Lett.* **88**, 082904 (2006).

¹⁴K. Szot, W. Speier, G. Bihlmayer, and R. Waser, *Nature Mater.* **5**, 312 (2006).

¹⁵R. Meyer, L. Schloss, J. Brewer, R. Lambertson, W. Kinney, J. Sanchez, and D. Rinerson, *Proceedings IEEE Non-Volatile Memory Technology Symposium (IEEE, Pacific Grove, CA, 2008)*, p. 1–5.

¹⁶Y. Z. Chen *et al.*, *Nat. Commun.* (to be published).